Identification method of non-reflective faults based on index distribution of optical fibers

Wonkyoung Lee,* Seung Il Myong, Jyung Chan Lee, and Sangsoo Lee

Optical Internet Research Department, Electronics and Telecommunications Research Institute, 161 Gajeong-dong, Yuseong-gu, Daejeon, 305-350, South Korea
wklee@etri.re.kr

Abstract: This paper investigates an identification method of non-reflective faults based on index distribution of optical fibers. The method identifies not only reflective faults but also non-reflective faults caused by tilted fiber-cut, lateral connector-misalignment, fiber-bend, and temperature variation. We analyze the reason why wavelength dependence of the fiber-bend is opposite to that of the lateral connector-misalignment, and the effect of loss due to temperature variation on OTDR waveforms through simulation and experimental results. This method can be realized by only upgrade of fault-analysis software without the hardware change, it is, therefore, competitive and cost-effective in passive optical networks.

OCIS codes: (060.2360) Fiber optics links and subsystems; (060.2330) Fiber optics communications.

References and links

1. K. Yuksel, V. Moeyaert, M. Wuilpart, and P. Megret, "Optical layer monitoring in passive optical networks (PONs): a review," in *Proceedings of International Conference on Transparent Optical Networks* (2008), Vol. 1, pp. 92–98.
2. A. E. Willner and Z. Q. Pan, "Optical characterization, diagnosis, and performance monitoring for PON," in *Passive Optical Networks Principles and Practice* (Academic, 2007), Chap. 7, pp. 267–300.
3. P. J. Urban, A. Getaneh, J. P. von der Weid, G. P. Temporao, G. Vall-llosera, and J. Chen, "Detection of Fiber Faults in Passive Optical Networks," J. Opt. Commun. Netw. **5**(11), 1111–1121 (2013).
4. K. Tsujikawa, M. Takaya, and S. Tomita, "Method for estimating loss over wide wavelength region of fiber cables installed in access networks," in *Proceedings of Optical Fiber Communication/National Fiber Optic Engineers Conference* (2010), JThA54.
5. T. Kurashima, M. Tateda, K. Shimizu, T. Horiguchi, and Y. Koyamada, "A high performance OTDR for measuring distributed strain and optical loss," in *Proceedings of European Conference on Optical Communication* (1996), Vol. 2, pp. 215–218.
6. W. Lee, J. C. Lee, S. I. Myong, and S. S. Lee, "Fault-Identification Method Based on Index Distribution of Optical Fibers for Enhanced Optical Link Monitoring," in *Proceedings of Optical Fiber Communication/National Fiber Optic Engineers Conference* (2013), NWIJ.4.
7. D. R. Anderson, L. M. Johnson, and F. G. Bell, "Fundamentals of fiber optics," in *Troubleshooting Optical Fiber Networks: Understanding and Using Optical Time Domain Reflectometer* (Academic, 2004), Chap. 2, pp. 13–58.
8. M. Heiblum and J. H. Harris, "Analysis of curved optical waveguides by conformal transformation," J. Quantum Electron. **11**(2), 75–83 (1975).
9. L. Dong, "Stimulated thermal Rayleigh scattering in optical fibers," Opt. Express **21**(3), 2642–2656 (2013).
10. A. Rostami and S. Makouei, "Temperature dependence analysis of the chromatic dispersion in WII-type zero-dispersion shifted fiber (ZDSF)," Prog. Electromagn. Res. B **7**, 209–222 (2008).
11. N. Ferrari, L. Greborio, F. Montalti, P. Regio, and G. Vespasiano, "OTDR characteristics for PON measurements," in *International Wire and Cable Symposium* (2008), pp. 27–35.

1. Introduction

The technical trends in today's passive optical network (PON) system have been focused in service integration, implementation of wavelength division multiplexing, high bit-rate and longer reach/higher split options. They all lead to capacity increase and make a network failure more disastrous [1]. PON infrastructure does not only suffer from accidental damage and environmental effects but are also subject to a lot of changes after the network is installed

#199797 - $15.00 USD Received 18 Oct 2013; revised 28 Nov 2013; accepted 15 Dec 2013; published 2 Jan 2014

and activated. Optical link management (OLM) in PONs has been gaining importance as the warranty on the quality of the infrastructure becomes a deciding factor in the strongly competitive marketplace. The optical link management should be able to timely detect, localize, and identify faults for operation-and-maintenance expenses (OPEX) savings. The OLM technology in the PON networks has mainly been realized using optical time domain reflectometry (OTDR) technique since the OTDR is well-suited technique for the location of fiber cable faults [2]. PON monitoring based on combined OTDR and optical transceiver monitoring has been proposed in 2011 to localize fault in the drop sections of PON system [3]. Kyozo Tsujikwa et al. have presented the method for estimating loss over wide wavelength region of fiber cables installed in access networks in 2010 [4]. The method predicts loss values at any wavelength from the measured loss values at only three or four wavelengths. For intelligent management of the physical layer such as continuous, remote, and automatic supervision, methods for identifying faults accurately have been studied steadily. In the conventional OTDR, the fault by the fiber-cut is identified comparatively easily by reflection peaks and the abrupt decrease of the reflection power in the OTDR trace. However, it is difficult to exactly identify non-reflective faults caused by lateral connector-misalignment, splicing loss, or fiber-bend. An identification method of non-reflective fault using a Brillion frequency shift induced by bending has been reported [5]. However, the method has a complex architecture and is difficult to implement in the real field. Recently, we have presented an identification method of faults of bending and connector mismatch [6]. The wavelength dependence of different non-reflective losses is a known phenomenon [7] however there is no detailed explanation. To the best of our knowledge, we have not found references that analyze variation of OTDR traces due to temperature change of an optical fiber.

In this paper, we investigate an identification method of non-reflective faults based on index distribution of optical fibers. We make the detailed explanation and arrange relations between loss mechanism and fault-identification methods. We analyze the variation of OTDR traces due to the temperature change for identifying fault's origin. And we verify the fault-identification method through simulation and experimental results. Motive of our study is to improve fault identification methods based on the fact that intrinsic properties of optical fibers such as index distribution, birefringence, and so on are changed differently according to event conditions. Section 2 explains OTDR waveforms of the reflective faults and the non-reflective faults. Sections 3, 4, and 5 describe the loss mechanism of bending, connector misalignment, and temperature variation in detail. Experimental results and discussion for the proposed method are presented in section 6. Finally the paper ends with a short conclusion. The method overcomes the limitation of the conventional fault-identification methods and is competitive and cost-effective because it can be realized by only upgrade fault analysis software without the hardware change.

2. Reflective faults and non-reflective faults

2.1 Reflective faults

Link management technology based on the OTDR technique identifies optical faults by sharp peak or/and attenuation in the OTDR trace. When a fiber is cut perpendicular to the cross section of the fiber as shown in Fig. 1(a), Fresnel reflection occurs because of the large difference of reflective index between the fiber's core and air. Consequently, a sharp peak and abrupt decrease of the reflection power down to the noise floor appear on an OTDR trace as shown in Fig. 1(c). In the case of the longitudinal connector-misalignment of Fig. 1(b), small peak occurs in the OTDR trace as shown in Fig. 1(c). Reflective faults are identified by characteristics of OTDR waveforms such as large peaks, abrupt decrease of power, small peaks, and attenuation of power.

#199797 - $15.00 USD Received 18 Oct 2013; revised 28 Nov 2013; accepted 15 Dec 2013; published 2 Jan 2014

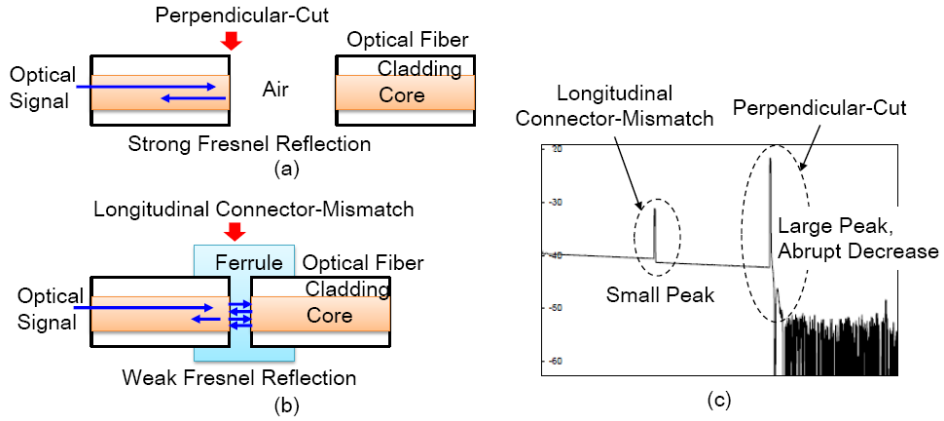

Fig. 1. Reflective faults: (a) perpendicular fiber-cut, (b) longitudinal connector-misalignment, and (c) OTDR traces of reflective faults.

2.2 Non-reflective faults

Non-reflective faults involve only attenuation of Rayleigh backscattering and no reflection. As shown in Fig. 2, the Rayleigh backscattering origins from various faults such as splicing error, fiber-bend, temperature variation, and so on. Non-reflective faults are not identified by the conventional OTDR analysis based on only OTDR trace because the faults generate the same OTDR waveform.

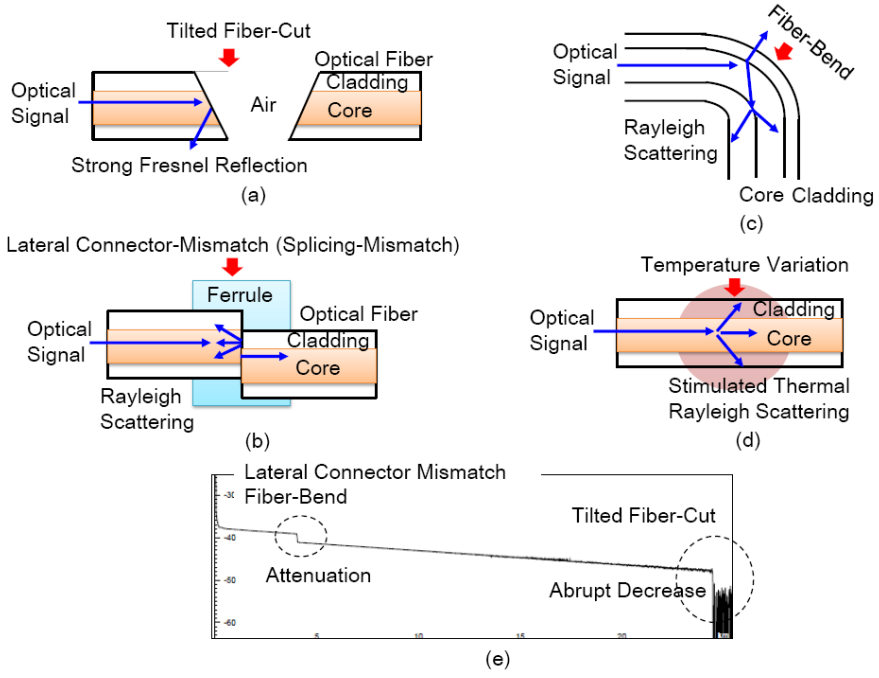

Fig. 2. Non-reflective faults: (a) tilted fiber-cut, (b) lateral connector-misalignment, (c) fiber-bend, (d) temperature variation, and (e) OTDR traces of non-reflective faults.

Figure 2 explains non-reflective faults and the corresponding OTDR waveform. In the tilted fiber-cut of Fig. 2(a), Fresnel reflection occurs, but there is no power reflected toward the OTDR because the reflected signal goes to orthogonal directions of the tilted end face. In the lateral misalignment of Fig. 2(b), only Rayleigh scattering without Fresnel reflection

#199797 - $15.00 USD Received 18 Oct 2013; revised 28 Nov 2013; accepted 15 Dec 2013; published 2 Jan 2014

occurs because of a small difference in the reflective index between a core of one fiber and a cladding of the opposite fiber. As shown in Figs. 2(c) and 2(d), bend and temperature induce index variation of optical fibers, so a portion of the optical power is lost. Among the listed faults, the lateral connector-misalignment, the fiber-bend, and the temperature variation are very difficult to distinguish because only smoothly decreased regions appear on the OTDR trace as shown in Fig. 2(e). In this paper, we propose fault-identification methods based on the index distribution of optical fibers that exactly identify the non-reflective faults.

3. Loss mechanism of the fiber-bend

3.1 Waveguide analysis in bent fibers

To exactly understand the loss mechanism in a bent fiber, we have investigated the change of index distribution in the bent fiber using the conformal transformation method. The conformal transformation is a method that analyzes curved waveguides by transforming the circularity curved fiber into an equivalent straight fiber as shown in Fig. 3 [8].

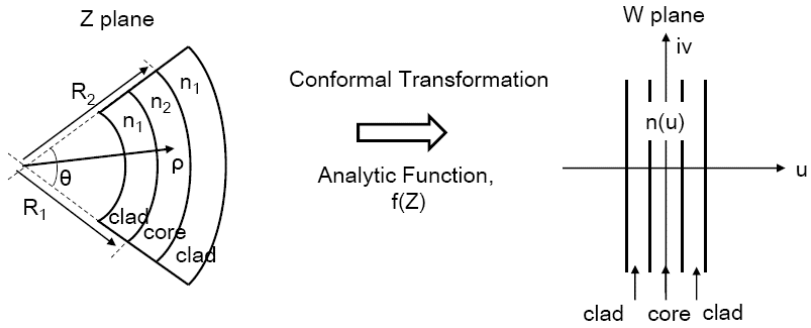

Fig. 3. Equivalent waveguide structures of curved optical waveguide via the conformal transformation method.

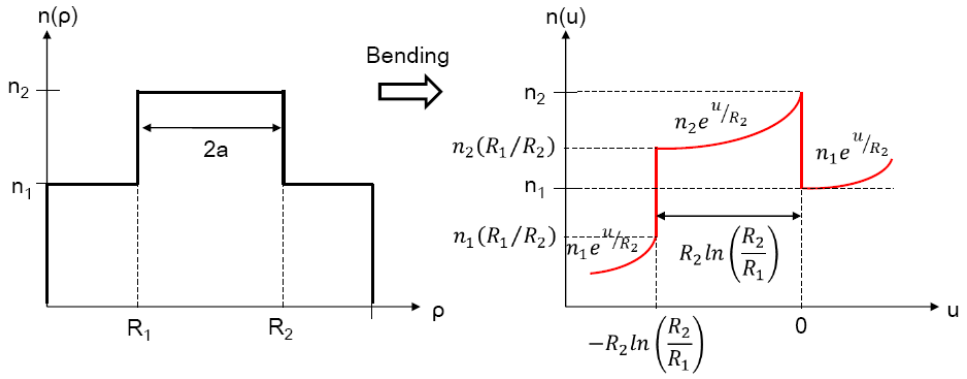

Fig. 4. Transformation of step index distribution in the curved optical waveguide.

Conformal transformations apply to solutions of the two-dimensional scalar wave equation [8].

$$\left[\nabla_{x,y}^2 + \kappa^2(x,y)\right]\Psi = 0 \tag{1}$$

Solutions are obtained in a coordinate system u, v defined with respect to x and y by the relation

$$W = u + iv = f(Z) = f(x + iy) \tag{2}$$

#199797 - $15.00 USD Received 18 Oct 2013; revised 28 Nov 2013; accepted 15 Dec 2013; published 2 Jan 2014

where f is an analytic function. Equation (1) may be expressed as

$$\left[\Delta_{u,v}^2 + \left|\frac{dZ}{dW}\right|^2 \kappa^2\left(x(u,v), y(u,v)\right)\right]\Psi = 0 \tag{3}$$

The transformation finds an f(Z) that converts curved boundaries in the x, y plane to straight ones in the u, v plane in Fig. 3.

$$f(Z) = W = R_2 \ln\frac{Z}{R_2} \tag{4}$$

for which

$$\left|\frac{dZ}{dW}\right| = \exp\left(u/R_2\right) \tag{5}$$

Figure 3 explains that the circularly curved waveguide with a step discontinuity in the refractive index at radii R_1 and R_2 in the Z plane is converted into the equivalent straight waveguide in the W plane where the wall are straight and lie between u = 0 and $u = -R_2 \ln(R_2/R_1)$. The step index profile in the straight fiber is distorted into the index profile of Fig. 4 by bending.

3.2 Simulation results for bending effect of optical fibers

Using the index transformation of bent fibers in the Fig. 4, we have simulated the distorted index distribution of the bent fiber with the following conditions: the core index of 1.467, the cladding index of 1.457, the core radius of 5-μm, bend radius (R_2) of 2-cm.

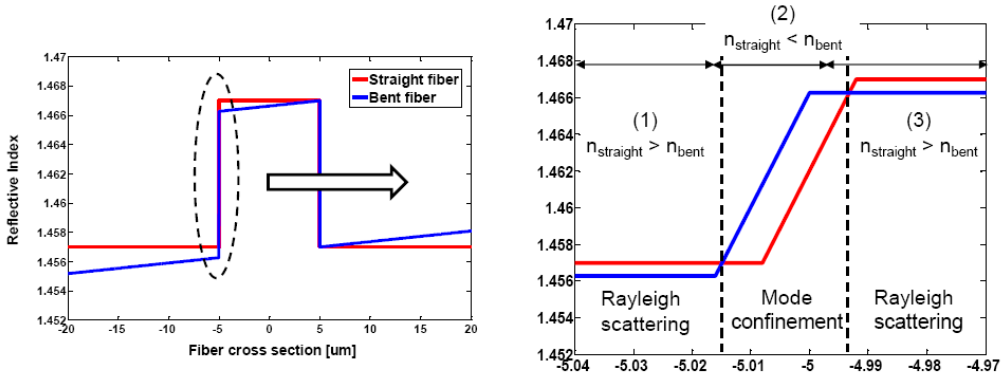

Fig. 5. Transformed index distribution of the bent fiber and enlarged views of the rising edge.

#199797 - $15.00 USD Received 18 Oct 2013; revised 28 Nov 2013; accepted 15 Dec 2013; published 2 Jan 2014

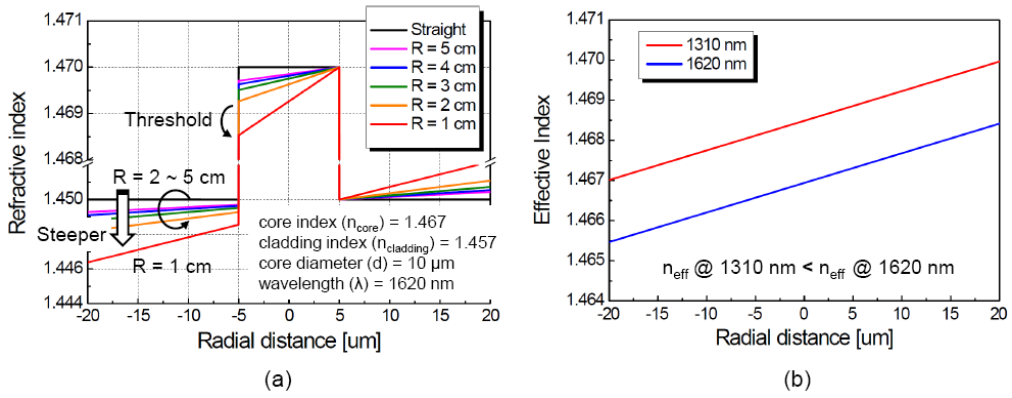

Fig. 6. (a) Effect of bend radius on the modified index profile, (b) Effective indices as function of wavelengths in the straight and bent fibers.

Figure 5 describes the transformed index distribution of a single mode fiber due to macro-bending with bending radius of 2 cm. Index distribution is changed from the step profile to the tilted profile by the fiber-bend. Because of mode confinement of the rising edge and the tilted profile in the Fig. 5, the beam intensity within the fiber is changed from a symmetrical pattern to a distorted shape. In the enlarged view of Fig. 5, loss by Rayleigh scattering in the core occurs due to a small decrease of the refractive index in the bent fiber. Figure 6(a) describes the effect of the bend radius on the modified index profile. Tilt of the modified index distribution steepens further as the bend radius becomes smaller. There is a threshold of the bending radius where the bending loss abruptly increases over the critical bend radius as shown in Fig. 6(a). Based on the above fact, the conventional OTDR estimates that the fault is caused by bending if loss is large, otherwise, the fault is caused by splicing error or connector mismatch [4]. Fault identification method of the convention OTDR is inaccurate and it makes a wrong estimate for small bending loss. Therefore, the objective of this paper is to propose an accurate fault identification method based on clear reason and fact. Figure 6(b) describes effective indices as function of wavelengths in the straight and bent fibers. As wavelengths are smaller, effective indices of the bent fiber become higher and then mode confinement in the core becomes to better preserve. For this reason, the light of shorter wavelength propagated within the fiber is less suffering from index distortion due to bending. The bending loss at longer wavelength is therefore larger than that at shorter wavelength and the relation of Eq. (6) can be formed.

$$\alpha_b\big|_{1310nm} < \alpha_b\big|_{1625nm} \tag{6}$$

where $\alpha_b\big|_{1310nm}$ and $\alpha_b\big|_{1625nm}$ are bending losses at 1310 nm and 1625 nm, respectively.

3.3 Experimental results for wavelength dependence of fiber-bend

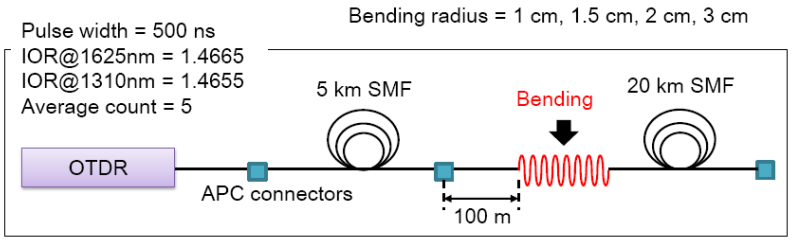

Fig. 7. Experimental setup for measuring the bending loss with bending radius of 1 cm, 1.5 cm, 2 cm, and 3 cm at 1310 nm and 1625 nm using OTDR technique.

#199797 - $15.00 USD Received 18 Oct 2013; revised 28 Nov 2013; accepted 15 Dec 2013; published 2 Jan 2014

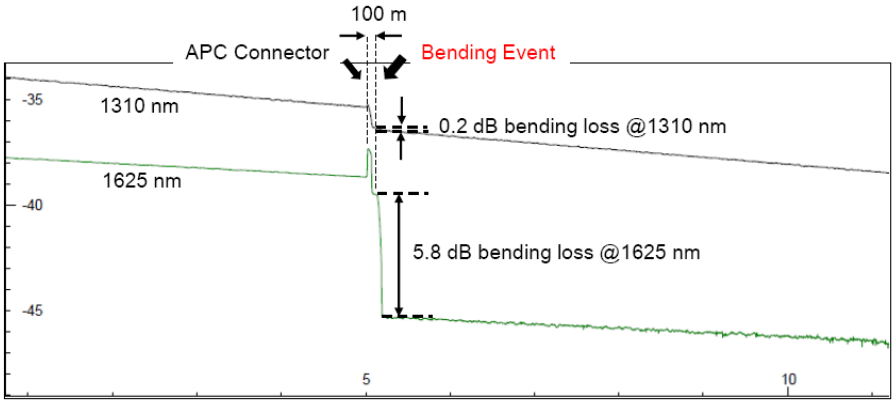

Fig. 8. Experimental results for bending loss with bending radius of 1.5 cm at 1310 nm and 1625 nm.

Figure 7 shows experimental setup for measuring the wavelength dependence of bending loss. The bending loss has measured at the two wavelengths of 1310 nm and 1625 nm using conventional OTDR equipment for bending radius of 1 cm, 1.5 cm, 2 cm, and 3 cm. The test link of Fig. 7 consists of an SMF spool of 5 km and an SMF spool of 20 km. Bending Events were applied at the midpoint of two fiber spools of 5 km SMF and 20 km SMF. The connector was placed in a distance of 100 m from the bending event corresponding to larger than the resolution of the measurement. The OTDR pulse width was 500 nm. Figure 8 shows OTDR traces measured at the two wavelengths of 1310 nm and 1625 nm in the event of fiber-bend with bending radius of 1.5 cm. The bending loss was calculated as the difference of reflected powers before and after the bending event. We have verified the fact that the bending loss at longer wavelength is larger than that at shorter wavelength and the experimental result is same as the expected result.

4. Loss mechanism of connector-misalignment

4.1 Simulation results for connector-misalignment effect

Loss due to the connector-misalignment originates from a mismatch between the mode field diameters (MFDs) of two fibers. The mode field diameter is the diameter at which power density is reduced to $1/e^2$ of the maximum power density (I_0) as shown in Fig. 9(a). Coupling loss is originated from lateral misalignment between two fibers. Coupling loss gradually increases as the lateral misalignment becomes larger and there is no threshold at which the loss abruptly increases. Figure 9(b) describes MFDs at three wavelengths of 1310 nm, 1550 nm, and 1625 nm. The MFD of the shorter wavelength is smaller than that of the longer wavelength. Therefore, loss due to the connector-misalignment at the shorter wavelength is larger than that at the longer wavelength and the relation between loss due to lateral connector-misalignment and wavelengths is as follows.

$$\alpha_c\big|_{1310nm} > \alpha_c\big|_{1625nm} \tag{7}$$

where $\alpha_c\big|_{1310nm}$ and $\alpha_c\big|_{1625nm}$ are connector losses at 1310 nm and 1625 nm, respectively.

#199797 - $15.00 USD Received 18 Oct 2013; revised 28 Nov 2013; accepted 15 Dec 2013; published 2 Jan 2014

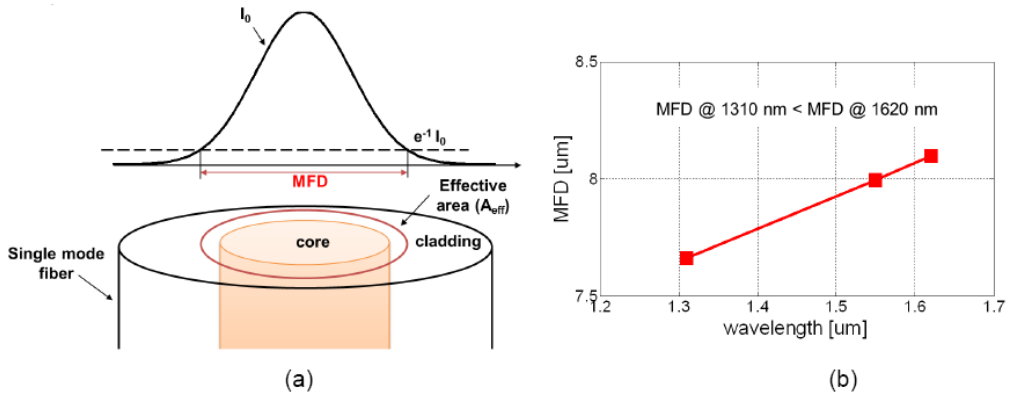

Fig. 9. (a) Definition of mode field diameter, (b) Wavelength dependences of MFD.

Wavelength dependence of loss due to the connector-misalignment is opposite to that of bending loss. The proposed fault-identification method uses the difference in wavelength dependences of the bending loss and the connector loss.

4.2 Experimental results for wavelength dependence of connector-misalignment

As shown in Fig. 10, the experimental setup for measuring the connector loss is similar with the experiment for measuring the bending loss of Fig. 7 excluding not fiber-bend but connector-misalignment. Through the experimental results of Fig. 11, we have confirmed that loss due to the connector-misalignment at the shorter wavelength is larger than that at the longer wavelength. This is same as the expected result.

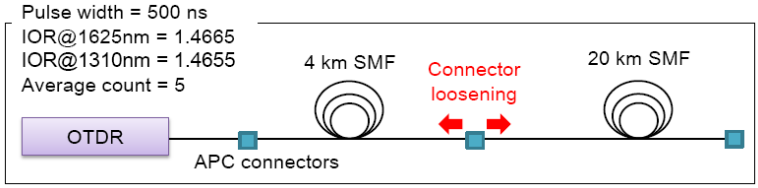

Fig. 10. Experimental setup for measuring the connector loss at 1310 nm and 1625 nm using OTDR.

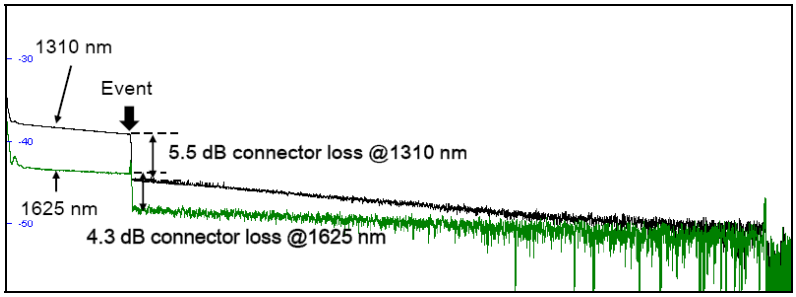

Fig. 11. Experimental results for connector loss at 1310 nm and 1625 nm.

5. Loss mechanism of temperature variation

5.1 Thermal effects in optical fibers

Local heating stimulates power coupling to the scattered light via thermal-optics effect called as stimulated thermal Rayleigh scattering (STRS) [9]. The backscattered signals are increased by positive temperature. Negative temperature prevents power coupling into the scattered

#199797 - $15.00 USD Received 18 Oct 2013; revised 28 Nov 2013; accepted 15 Dec 2013; published 2 Jan 2014

light and then reduces the backscattered signals. Attenuation in optical links is caused by large temperature variation as one of environmental effects. Moreover, large temperature variation induce power coupling to the scattered light and result in instability of propagated signal power. The refractive index variation due to temperature is expressed in terms of thermo-optic coefficient dn/dT [10]. It can be described in terms of a normalized wavelength $R = \lambda^2/(\lambda^2 - \lambda^2_g)$ as

$$2n\left(\frac{dn}{dT}\right) = GR + HR^2 = G\left(\frac{\lambda^2}{\lambda^2 - \lambda_g^2}\right) + H\left(\frac{\lambda^2}{\lambda^2 - \lambda_g^2}\right)^2 \tag{8}$$

where the constants G and H are related respectively to the thermal expansion coefficient (α) and the energy gap temperature coefficient. Figure 12 shows the thermo-optic coefficient versus wavelength for silica glasses. Thermo-optic coefficient gradually increases as wavelengths decrease according to the Eq. (8) presented in [10]. Fluctuation of Backscattered power at shorter wavelength is larger than that of longer wavelength.

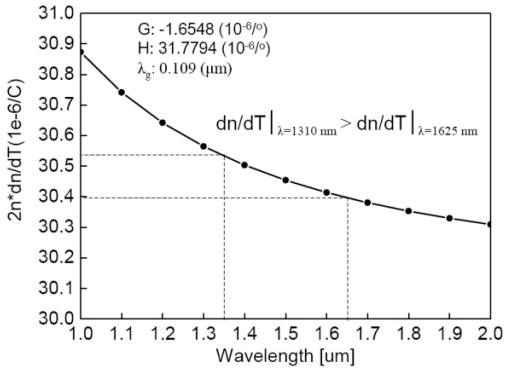

Fig. 12. Thermo-optic coefficient versus wavelengths for silica glasses.

5.2 Experimental results for temperature variation

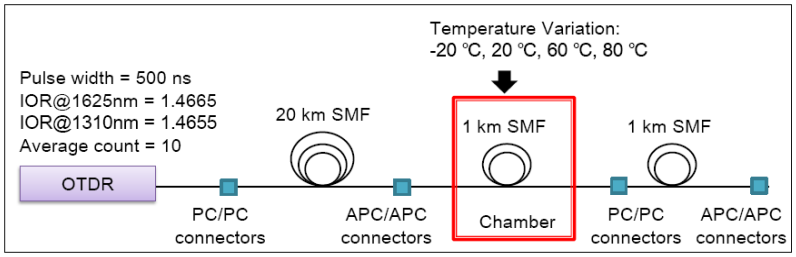

Fig. 13. Experimental setup for measuring the loss due to temperature variations of −20 °C, 20 °C, 60 °C, and 80 °C at 1310 nm and 1625 nm using OTDR.

Figure 13 describes experimental setup for measuring the loss due to temperature variation at two wavelengths of 1310 nm and 1625 nm. The test link consists of an SMF spool of 20 km and two SMF spools of 1 km. To apply the event of temperature variation, one of two SMF spools of 1 km put into a chamber, whose temperature was controlled from −20 °C to 80 °C.

#199797 - $15.00 USD Received 18 Oct 2013; revised 28 Nov 2013; accepted 15 Dec 2013; published 2 Jan 2014

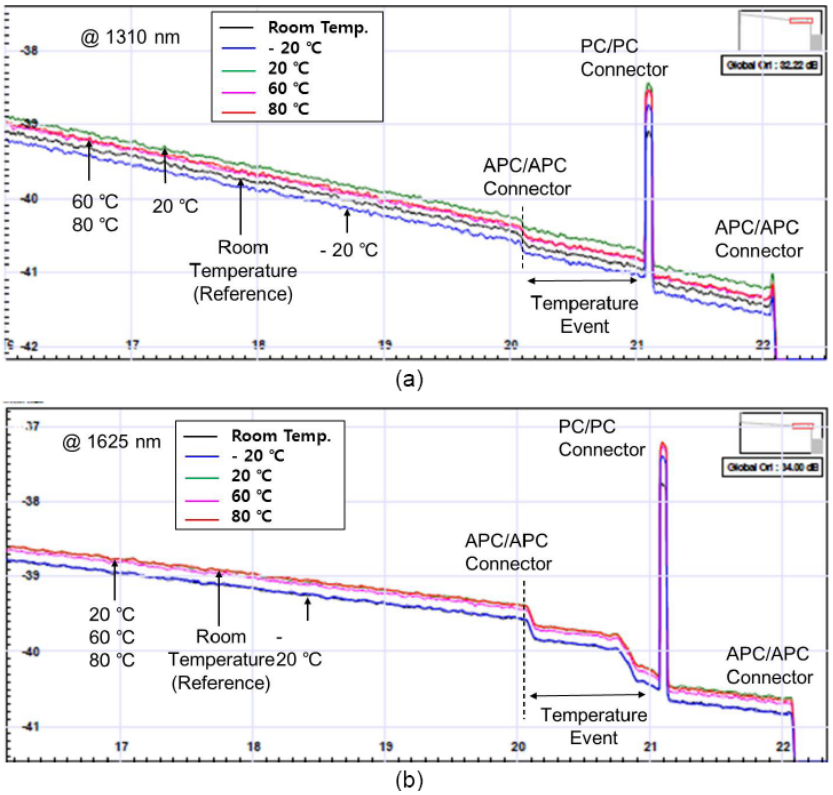

Fig. 14. Measured OTDR traces with temperature of –20 °C, 20 °C, 60 °C, and 80 °C at two wavelengths of (a) 1310 nm and (b) 1625 nm.

We have measured OTDR traces with temperature of –20 °C, 20 °C, 60 °C, and 80 °C at two wavelengths of 1310 nm and 1625 nm. In case of high temperature variation, linear slope of the OTDR trace was shifted up and down as shown in Fig. 14. This characteristic of the temperature variation is different from characteristics of fiber-bend and connector-misalignment. With positive temperature of 20 °C, 60 °C, and 80 °C, linear slope of the OTDR trace was moved up compared to that with room temperature. On the other hand, linear slope of the OTDR trace with negative temperature of –20 °C was moved down.

6. Proposed fault-identification based on index distribution

Figure 15 shows the comparison for the wavelength dependences of the bend loss and the connector loss. From Fig. 15, we have verified three points. At first, the bending loss at 1625 nm (hollow circle) is larger than that at 1310 nm (black square) as shown in Fig. 15(a). However, the connector loss at 1625 nm (hollow circle) is smaller than that at 1310 nm (black square) as shown in Fig. 15(b). At second, the difference of bending loss at 1310 nm and 1625 nm gets bigger, as the bending loss becomes larger. However, the difference of connector loss at 1310 nm and 1625 nm is much smaller compared to that of the bending loss. At third, there is a threshold in the pattern of the bending loss at 1625 nm. On the other hand, there is no threshold in the pattern of the connector loss at 1625 nm.

#199797 - $15.00 USD Received 18 Oct 2013; revised 28 Nov 2013; accepted 15 Dec 2013; published 2 Jan 2014

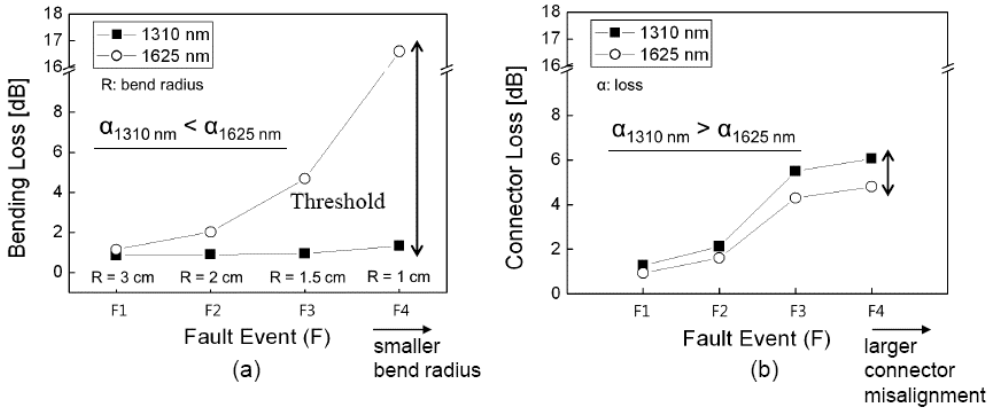

Fig. 15. Experimental results for wavelength dependence of (a) bending loss and (b) connector loss.

Table 1 describes features of the enhanced fault-identification method based on index distribution. The method is focused on identifying non-reflective faults such as tilted fiber-cut, fiber-bend, lateral connector-misalignment, and temperature variation. In the proposed fault analysis method, reflective faults are identified as perpendicular fiber-cut from sharp peak and abrupt decrease, or as longitudinal connector-misalignment from small peak on the OTDR waveform. Especially, non-reflective faults are classified as tilted fiber-cut from no peak and abrupt decrease, or as fiber-bend from no peak, small decrease, and small loss at the short wavelength compared to the longer wavelength, or as lateral connector-misalignment from no peak, small decrease, and large loss at the short wavelength compared to the longer wavelength, or as temperature variation from no peak and linear slope shift.

Table 1. Comparison between the proposed fault analysis method and conventional method

OTDR Events	OTDR Waveform		Fault Identification	Conventional Method*	Proposed Method
Reflective Event	Sharp Peak, Abrupt Decrease		Perpendicular Fiber-Cut	○	○
	Small Peak		Longitudinal Connector-Misalignment	○	○
Non-Reflective Event	No Peak, Abrupt Decrease		Tilted Fiber-Cut	○	○
	No Peak, Small Decrease	$\alpha_s < \alpha_l$	Fiber-Bend	X	○
		$\alpha_s > \alpha_l$	Lateral Connector-Misalignment	X	○
	No Peak, Linear Slope Shift		Temperature Variation	X	○

* Conventional method is the fault analysis method based on OTDR signal waveforms only.

The detailed explanation of the proposed method shows in Fig. 16. The fault-identification method generates OTDR loss trace by subtracting initial OTDR trace without a fault from present OTDR trace with a fault. On the OTDR loss trace, it checks whether there is abrupt decrease down to noise floor or not. If there are abrupt decrease and a peak at faulty location, it identifies OTDR event as reflective event and fault cause as perpendicular fiber-cut. If there is abrupt decrease but no peak at faulty location, it identifies OTDR event as non-reflective event and fault cause as tilted fiber-cut. The faults corresponding to the perpendicular fiber-cut and tilted fiber-cut are critical alarm and should be notified to operator or external maintenance system (EMS). In case of no abrupt decrease down to noise floor, if there is a peak at faulty location, it identifies OTDR event as reflective event and fault cause as

#199797 - $15.00 USD Received 18 Oct 2013; revised 28 Nov 2013; accepted 15 Dec 2013; published 2 Jan 2014

connector misalignment. If there are no abrupt decrease and slope shift of loss trace, it identifies OTDR event as non- reflective event and fault cause as temperature variation. If there are no abrupt decrease and no peak, it identifies fault cause as fiber-bend or connector misalignment according to wavelength dependence of loss.

```
OTDR loss trace
= present trace (with faults) – initial trace (without faults)

On the OTDR loss trace,

/* Fault-identification for fiber-cut */
if (abrupt decrease down to noise floor) {
    if ( a peak at faulty location)  {
        OTDR event = Reflective event
        Fault cause = Perpendicular fiber-cut
    }
    else  {
        OTDR event = Non-reflective event
        Fault cause = Tilted fiber-cut
    }

    Fault alarm = Critical alarm (Link failure)
    Notify the fault alarm to network operator or EMS
}
```

```
/* Fault-identification for connector--misalignment,
   fiber-bend, temperature variation */
else {
    if (a peak at faulty location)  {
        OTDR event = Reflective event
        Fault cause = Longitudinal connector-misalignment
        if (loss > max. threshold)
            Fault alarm = Critical alarm (Link failure)
        else if (min. threshold < loss < max. threshold)
            Fault alarm = Major alarm (Link attenuation)
        else
            Fault alarm = Minor alarm / warning
    }
    else if (slope shift of the loss trace) {
        OTDR event = Non-reflective event
        Fault cause = Temperature Variation
        Fault alarm = warning (performance degradation)
    }
    else  {
        OTDR event = Non-reflective event
        if (α_s < α_i)
            Fault cause = Fiber-bend
        else if (α_s > α_i)
            Fault cause = Lateral connector-misalignment
        if (loss > max. threshold)
            Fault alarm = Critical alarm (Link failure)
        else if (min. threshold < loss < max. threshold)
            Fault alarm = Major alarm (Link attenuation)
        else
            Fault alarm = warning (performance degradation)
    }

    Notify the fault alarm to network operator or EMS
}
```

Fig. 16. Detailed explanation of the proposed method.

7. Discussion

It is fundamental problems of PON monitoring to distinguish faulty branches after the passive splitter and localize the faults. A common method for distinguishing faulty branches in TDM PON is to place ONU branches in different distances from the passive splitter in order that peaks corresponding to the end positions of ONU branches don't overlay each other on an OTDR trace [11]. Our approach resolves the problem of identifying fault's cause and is capable to apply in PON monitoring since the wavelength dependence of loss is intrinsic property of the optical fiber and the property is not changed according to link architectures such as point to point link and point to multipoint link. A faulty branch can be detected by comparing between present OTDR trace with a fault and initial OTDR trace without a fault. And then, causes of the fault are identified by applying the proposed method in the faulty branch. It is possible to solve the fundamental problems of PON monitoring such as fault detection, identification, and localization by realizing the fault-identification method proposed in this study and the method, mentioned above, distinguishing faulty branches together.

Link monitoring based on OTDR has actively been investigating in PON application for real-time link monitoring. Although the experiment of our paper was not point to multipoint link but point to point link, the proposed fault identification is suitable in PON application because our approach can result in OPEX saving by improving fault analysis performance while it does not affect hardware performance of the PON monitoring such as resolution and dynamic range.

#199797 - $15.00 USD Received 18 Oct 2013; revised 28 Nov 2013; accepted 15 Dec 2013; published 2 Jan 2014

8. Conclusion

We have proposed the identification method of non-reflective faults such as fiber-cut, connector-misalignment, fiber-bend, and temperature variation. We have analyzed the reason why wavelength dependence of the fiber-bend is opposite to that of the lateral connector-misalignment. As wavelengths are smaller, effective indices of the bent fiber become higher and mode confinement in the core becomes to better preserve. Therefore, the light of shorter wavelength propagated within the fiber is less suffering from index distortion due to bending. The bending loss at longer wavelength is larger than that at shorter wavelength. Loss due to the connector-misalignment that originates from a mismatch between the mode field diameters (MFDs) of two fibers, at the shorter wavelength is larger than that at the longer wavelength because the MFD of the shorter wavelength is smaller than that of the longer wavelength. We measured the effect of loss due to temperature variation from –20 °C to 80 °C on OTDR waveforms at two wavelengths of 1310 nm and 1625 nm. In case of high temperature variation, linear slopes of the OTDR traces are shifted up and down, this result is quite different from the faults of fiber-bend and connector-misalignment

In the conventional method, it has been difficult to identify the non-reflective faults caused by tilted fiber-cut, lateral connector-misalignment, fiber-bend, and temperature variation because all OTDR traces are same. The proposed method resolves this shortage of the conventional method and is competitive and cost-effective because it can be realized by only upgrade fault analysis software without the hardware change. Our approach could contribute to improve fault identification of the intelligent optical link management equipped with optical test and diagnostic subsystem that manage optical link performance monitoring and manage OTDR testing. The optical test and diagnostic subsystem collects and analyzes measured link-monitoring data, determine fiber attenuation and identify reflection/attenuation event, and diagnose optical link fault condition.

Acknowledgments

This work was supported by the IT R&D program of MSIP/KEIT. [10041954, PON Transceiver with Real-Time OTDR function]

#199797 - $15.00 USD Received 18 Oct 2013; revised 28 Nov 2013; accepted 15 Dec 2013; published 2 Jan 2014